10

The Generalized Finite Element Method Applied to Free Vibration of Framed Structures

Marcos Arndt[1], Roberto Dalledone Machado[2] and Adriano Scremin[2]
[1]*Positivo University,*
[2]*Federal University of Paraná*
Brazil

1. Introduction

The vibration analysis is an important stage in the design of mechanical systems and buildings subject to dynamic loads like wind and earthquake. The dynamic characteristics of these structures are obtained by the free vibration analysis.

The Finite Element Method (FEM) is commonly used in vibration analysis and its approximated solution can be improved using two refinement techniques: *h* and *p*-versions. The *h*-version consists of the refinement of element mesh; the *p*-version may be understood as the increase in the number of shape functions in the element domain without any change in the mesh. The conventional *p*-version of FEM consists of increasing the polynomial degree in the solution. The *h*-version of FEM gives good results for the lowest frequencies but demands great computational cost to work up the accuracy for the higher frequencies. The accuracy of the FEM can be improved applying the polynomial *p* refinement.

Some enriched methods based on the FEM have been developed in last 20 years seeking to increase the accuracy of the solutions for the higher frequencies with lower computational cost. Engels (1992) and Ganesan & Engels (1992) present the Assumed Mode Method (AMM) which is obtained adding to the FEM shape functions set some interface restrained assumed modes. The Composite Element Method (CEM) (Zeng, 1998a and 1998b) is obtained by enrichment of the conventional FEM local solution space with non-polynomial functions obtained from analytical solutions of simple vibration problems. A modified CEM applied to analysis of beams is proposed by Lu & Law (2007). The use of products between polynomials and Fourier series instead of polynomials alone in the element shape functions is recommended by Leung & Chan (1998). They develop the Fourier *p*-element applied to the vibration analysis of bars, beams and plates. These three methods have the same characteristics and they will be called enriched methods in this chapter. The main features of the enriched methods are: (a) the introduction of boundary conditions follows the standard finite element procedure; (b) hierarchical *p* refinements are easily implemented and (c) they are more accurate than conventional *h* version of FEM.

At the same time, the Generalized Finite Element Method (GFEM) was independently proposed by Babuska and colleagues (Melenk & Babuska, 1996; Babuska et al., 2004; Duarte et al., 2000) and by Duarte & Oden (Duarte & Oden, 1996; Oden et al., 1998) under the following names: Special Finite Element Method, Generalized Finite Element Method, Finite Element Partition of Unity Method, *hp* Clouds and Cloud-Based *hp* Finite Element Method.

Actually, several meshless methods recently proposed may be considered special cases of this method. Strouboulis et al. (2006b) define otherwise the subclass of methods developed from the Partition of Unity Method including *hp* Cloud Method of Oden & Duarte (Duarte & Oden, 1996; Oden et al., 1998), the eXtended Finite Element Method (XFEM) of Belytschko and co-workers (Sukumar et al, 2000 and 2001), the Generalized Finite Element Method (GFEM) of Strouboulis et al. (2000 and 2001), the Method of Finite Spheres of De & Bathe (2001), and the Particle-Partition of Unity Method of Griebel & Schweitzer (Schweitzer, 2009). The GFEM, which was conceived on the basis of the Partition of Unity Method, allows the inclusion of a priori knowledge about the fundamental solution of the governing differential equation. This approach ensures accurate local and global approximations. Recently several studies have indicated the efficiency of the GFEM and others methods based on the Partition of Unity Method in problems such as analysis of cracks (Xiao & Karihaloo, 2007; Abdelaziz & Hamouine, 2008; Duarte & Kim, 2008; Nistor et al., 2008), dislocations based on interior discontinuities (Gracie et al., 2007), large deformation of solid mechanics (Khoei et al., 2008) and Helmholtz equation (Strouboulis et al., 2006a; Strouboulis et al., 2008). In structural dynamics, the Partition of Unity Method was applied by De Bel et al. (2005), Hazard & Bouillard (2007) to numerical vibration analysis of plates and by Arndt et al. (2010) to free vibration analysis of bars and trusses. Among the main challenges in developing the GFEM to a specific problem are: (a) choosing the appropriate space of functions to be used as local approximation and (b) the imposition of essential boundary conditions, since the degrees of freedom used in GFEM generally do not correspond to the nodal ones. In most cases the imposition of boundary conditions is achieved by the degeneration of the approximation space or applying penalty or Lagrange multipliers methods.

The purpose of this chapter is to present a formulation of the GFEM to free vibration analysis of framed structures. The proposed method combines the best features of GFEM and enriched methods: (a) efficiency, (b) hierarchical refinements and (c) the introduction of boundary conditions following the standard finite element procedure. In addition the enrichment functions are easily obtained. The GFEM elements presented can be used in plane free vibration analysis of rods, shafts, Euler Bernoulli beams, trusses and frames. These elements can be simply extended to spatial analysis of framed structures. The main features of the GFEM are discussed and the partition of unity functions and the local approximation spaces are presented. The GFEM solution can be improved using three refinement techniques: *h*, *p* and adaptive versions. In the adaptive GFEM, trigonometric and exponential enrichment functions depending on geometric and mechanical properties of the elements are added to the conventional Finite Element Method shape functions by the partition of unity approach. This technique allows an accurate adaptive process that converges very fast and is able to refine the frequency related to a specific vibration mode even for a coarse discretization scheme.

In this chapter the efficiency and convergence of the proposed method for vibration analysis of framed structures are checked. The frequencies obtained by the GFEM are compared with those obtained by the analytical solution, the CEM and the *h* and *p* versions of the Finite Element Method.

The chapter is structured as follows. Section 2 describes the variational form of the free vibration problems of bars and Euler-Bernoulli beams. The enriched methods proposed for free vibration analysis of bars and beams are discussed in Section 3. In Section 4 the main features of the GFEM and the formulation of C^0 and C^1 elements are discussed. Section 5 presents some applications of the proposed GFEM. Section 6 concludes the chapter.

2. Structural free vibration problem

Generally the structural free vibration problems are linear eigenvalue problems that can be described by: find a pair (λ, u) so that

$$Tu = \lambda Qu \text{ on } \Omega \text{, with} \tag{1}$$

$$Pu = 0 \text{ on } \partial\Omega \tag{2}$$

where T, Q and P are linear operators and $\partial\Omega$ corresponds to the boundary of domain Ω. The vibration of bars, stationary shafts and Euler-Bernoulli beams are mathematically modeled by elliptic boundary value problems, so T is a linear elliptic operator of order $2m$ and P is a consistent boundary operator of order m. Moreover, as the structural free vibration problems are derived from conservative laws, the operator T is formally assumed self-adjoint (Carey & Oden, 1983).

According to Carey & Oden (1984), in order to obtain the variational form of a time dependent problem, one should consider the time t as a real parameter and develop a family of variational problems in t. This consists in selecting test functions w, independent of t, and applying the weighted-residual method.

By this technique the structural free vibration problem becomes an eigenvalue problem with variational statement: find a pair (λ, u), with $u \in H(\Omega)$ and $\lambda \in \mathbf{R}$, so that

$$B(u,w) = \lambda F(u,w)\ ,\ \forall w \in H \tag{3}$$

where $B: H \times H \mapsto \mathbf{R}$ and $F: H \times H \mapsto \mathbf{R}$ are bilinear forms.

In numerical methods, finite dimensional subspaces of approximation $H^h \subset H(\Omega)$ are chosen and the variational statement becomes: find $\lambda_h \in \mathbf{R}$ and $u_h \in H^h(\Omega)$ so that

$$B(u_h,w) = \lambda_h F(u_h,w)\ ,\ \forall w \in H^h\ . \tag{4}$$

Established an overview of the problem, in what follows the specific features of the free vibration problems of bars and beams are presented.

2.1 Axial vibration of a straight bar

The bar consists of a straight rod with axial strain (Fig. 1). The basic hypotheses concerning physical modeling of bar vibration are (Craig, 1981): (a) the cross sections which are straight and normal to the axis of the bar before deformation remain straight and normal after deformation; and (b) the material is elastic, linear and homogeneous.

The momentum equation that governs this problem is the partial differential equation

$$\rho A(x)\frac{\partial^2 \bar{u}}{\partial t^2} - \frac{\partial}{\partial x}\left(EA(x)\frac{\partial \bar{u}}{\partial x}\right) = p(x,t) \tag{5}$$

where $A(x)$ is the cross section area, E is the Young modulus, ρ is the specific mass, p is the externally applied axial force per unit length and t is the time. The problem of free vibration is stated as: find the axial displacement $\bar{u} = \bar{u}(x,t)$ which satisfies Eq. (5) when $p(x,t) = 0$.

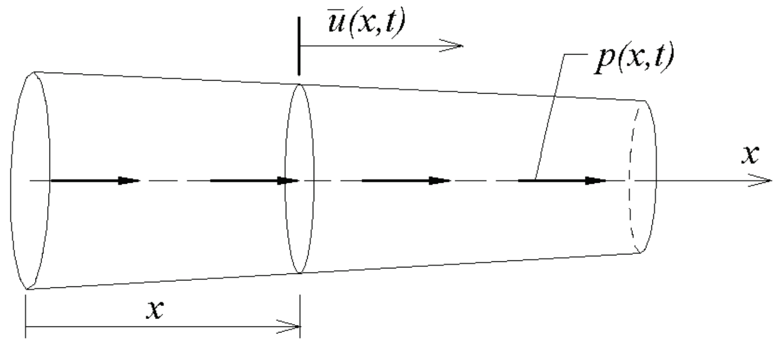

Fig. 1. Straight bar

Assuming periodic solutions $\overline{u}(x,t) = e^{i\omega\, t}u(x)$, where ω is the natural frequency, the free vibration of a bar becomes an eigenvalue problem with variational statement: find a pair (λ, u), with $u \in H^1(0,L)$ and $\lambda \in \mathbf{R}$, which satisfies Eq. (3) when H space is $H^1(0,L)$, $\lambda = \omega^2$ and L is the bar length.

The bilinear forms B and F in Eq. (3) for Dirichlet and Neumann boundary conditions are

$$B(u,w) = \int_0^L EA \frac{du}{dx}\frac{dw}{dx} dx \tag{6}$$

$$F(u,w) = \int_0^L \rho A u w dx \tag{7}$$

Similarly the bilinear forms for general natural boundary conditions are

$$B(u,w) = \int_0^L EA \frac{du}{dx}\frac{dw}{dx} dx + k_L u(0)w(0) + k_R u(L)w(L) \tag{8}$$

$$F(u,w) = \int_0^L \rho A u w dx + m_L u(0)w(0) + m_R u(L)w(L) \tag{9}$$

where k_L and k_R are the spring stiffness at left and right bar ends, respectively, and m_L and m_R are the masses at left and right bar ends, respectively.

The torsional free vibration of a circular shaft is mathematically identical to the axial free vibration of a straight bar so the variational forms of these problems are the same.

2.2 Transversal vibration of an Euler-Bernoulli beam

Consider a straight beam with lateral displacements, as illustrated in Fig. 2. The basic hypotheses concerning physical modeling of Euler-Bernoulli beam vibration are: (a) there is a neutral axis undergoing no extension or contraction; (b) cross sections in the undeformed beam remain plane and perpendicular to the deformed neutral axis, that is, transverse shear deformation is neglected; (c) the material is linearly elastic and the beam is homogeneous at any cross section; (d) normal stresses σ_y and σ_z are negligible compared to the axial stress σ_x ; and (e) the beam rotary inertia is neglected.

The momentum equation governing this problem is the partial differential equation

$$\frac{\partial^2}{\partial x^2}\left(EI\frac{\partial^2\overline{v}}{\partial x^2}\right)+\rho A\frac{\partial^2\overline{v}}{\partial t^2}=p(x,t) \tag{10}$$

where $I(x)$ is the second moment of area, $A(x)$ is the cross section area, E is the Young modulus, ρ is the specific mass, p is the externally applied transversal force per unit length and t is the time. The free vibration problem consists in finding the lateral displacement $\overline{v}=\overline{v}(x,t)$ which satisfies Eq. (10) when $p(x,t)=0$.
Assuming periodic solutions $\overline{v}(x,t)=e^{i\omega t}v(x)$, where ω is the natural frequency, the free vibration of a beam becomes an eigenvalue problem with variational statement: find a pair (λ,v), with $v\in H^2(0,L)$ and $\lambda\in\mathbf{R}$, which satisfies Eq. (3) when H space is $H^2(0,L)$, $\lambda=\omega^2$, $u=v$ and L is the beam length.

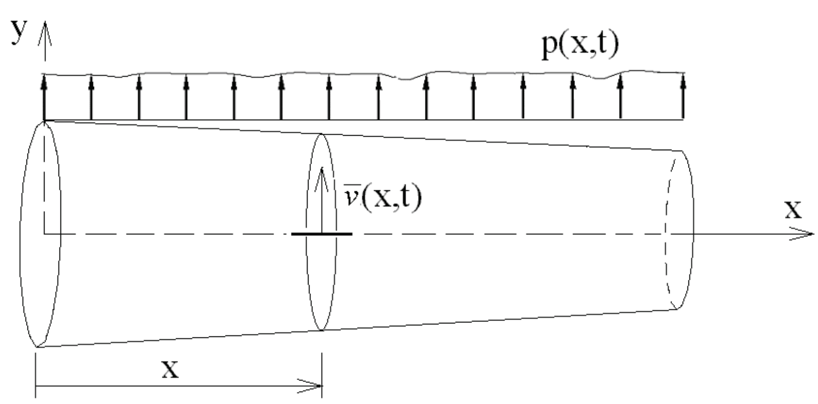

Fig. 2. Straight Euler-Bernoulli beam

For Dirichlet and Neumann boundary conditions the bilinear forms B and F in Eq. (3) are obtained from

$$B(v,w)=\int_0^L EI\frac{d^2v}{dx^2}\frac{d^2w}{dx^2}dx \tag{11}$$

$$F(v,w)=\int_0^L \rho Avw dx\,. \tag{12}$$

Similarly the bilinear forms for general natural boundary conditions are

$$\begin{aligned}B(v,w)=&\int_0^L EI\frac{d^2v}{dx^2}\frac{d^2w}{dx^2}dx+k_{TL}v(0)w(0)+k_{TR}v(L)w(L)+k_{RL}\left.\frac{dv}{dx}\right|_{x=0}\left.\frac{dw}{dx}\right|_{x=0}+\\&+k_{RR}\left.\frac{dv}{dx}\right|_{x=L}\left.\frac{dw}{dx}\right|_{x=L}\end{aligned} \tag{13}$$

$$\begin{aligned}F(v,w)=&\int_0^L \rho Avw dx+m_Lv(0)w(0)+m_Rv(L)w(L)+I_{mL}\left.\frac{dv}{dx}\right|_{x=0}\left.\frac{dw}{dx}\right|_{x=0}+\\&+I_{mR}\left.\frac{dv}{dx}\right|_{x=L}\left.\frac{dw}{dx}\right|_{x=L}\end{aligned} \tag{14}$$

where k_{TL}, k_{RL}, m_L and I_{mL} are translational stiffness, rotational stiffness, concentrated mass and moment of inertia of the attached mass at the left beam end, respectively, and k_{TR}, k_{RR}, m_R and I_{mR} are translational stiffness, rotational stiffness, concentrated mass and moment of inertia of the attached mass at the right beam end, respectively.

3. Enriched methods

Several methods found in the literature have as main feature the enrichment of the shape functions space of the classical FEM by adding other non polynomial functions. In this chapter such methods will be called enriched methods. Actually the Assumed Mode Method (AMM) of Ganesan & Engels (1992), the Composite Element Method (CEM) of Zeng (1998a, b and c) and the Fourier *p*-element of Leung & Chan (1998) are enriched methods. Their main features are: (a) the introduction of boundary conditions follows the standard finite element procedure; (b) hierarchical *p* refinements are easily implemented and (c) they present more accurate results than conventional *h*-version of FEM.
The approximated solution of the enriched methods, in the element domain, is obtained by:

$$u_h^e = u_{FEM}^e + u_{ENRICHED}^e \tag{15}$$

or in matrix shape

$$u_h^e = \mathbf{N}^T\mathbf{q} + \mathbf{Ø}^T\bar{\mathbf{q}} \tag{16}$$

where u_{FEM}^e is the FEM displacement field based on nodal degrees of freedom, $u_{ENRICHED}^e$ is the enriched displacement field based on field degrees of freedom, $\mathbf{q}$ is the conventional FEM degrees of freedom vector, the vector $\mathbf{N}$ contains the classical FEM shape functions and the vectors $\mathbf{Ø}$ and $\bar{\mathbf{q}}$ contain the enrichment functions and the field degrees of freedom, respectively. The vectors $\mathbf{Ø}$ and $\bar{\mathbf{q}}$ can be defined by:

$$\bar{\mathbf{Ø}}^{\mathrm{T}}(\xi) = \begin{bmatrix} F_1 & F_2 & \dots & F_r & \dots & F_n \end{bmatrix} \tag{17}$$

$$\bar{\mathbf{q}}^T = \begin{bmatrix} c_1 & c_2 & \cdots & c_n \end{bmatrix} \tag{18}$$

$$\xi = \frac{x}{L_e} \tag{19}$$

where F_r are the enrichment functions, c_r are the field degrees of freedom and L_e is the element length. Different sets of enrichment functions produce different enriched methods. The enrichment functions spaces of the main enriched methods are described as follows.

3.1 Enriched C^0 elements

C^0 elements are used in free vibration analysis of bars and shafts. In this section the enriched C^0 elements are described. In all these enriched methods the FEM displacement field corresponds to the classical FEM with two node elements and linear Lagrangian shape functions. Only the enrichment functions are different.
In the AMM proposed by Engels (1992) the enrichment functions are the normalized analytical solutions of the free vibration problem of a fixed-fixed bar in the form

$$F_r = C\,\sin\left(r\pi\xi\right), \quad r = 1,2,\ldots \tag{20}$$

where C is the mass normalization constant given by

$$C = \sqrt{\frac{2}{\rho A L_e}}\,. \tag{21}$$

The CEM enrichment functions proposed by Zeng (1998a) are trigonometric functions in the form

$$F_r = \sin\left(r\pi\xi\right), \quad r = 1,2,\ldots \tag{22}$$

They differ from those of AMM just by the normalization.
The enrichment functions used by Leung & Chan (1998) in the bar Fourier *p*-element and by Zeng (1998a) in the CEM are the same.
It is noteworthy that all these functions vanish at element nodes. This feature allows the introduction of boundary conditions following the standard finite element procedure.

3.2 Enriched C^1 elements

C^1 elements are used in free vibration analysis of Euler-Bernoulli beams. In this section the enriched C^1 elements are described. The FEM displacement field in these enriched methods corresponds to the classical FEM with two node elements and cubic Hermitian shape functions. The enrichment functions are described below.
In the AMM three different enrichment functions are proposed. Engels (1992) uses analytical free vibration normal modes of a clamped-clamped beam in the classical form

$$F_r = C_r\left\{\,\sinh\left(\lambda_r\xi\right) - \sin\left(\lambda_r\xi\right) - \alpha_r\left[\cosh\left(\lambda_r\xi\right) - \cos\left(\lambda_r\xi\right)\right]\,\right\} \tag{23}$$

$$C_r = \frac{1}{\sqrt{\rho A L_e \alpha_r^2}} \tag{24}$$

$$\alpha_r = \frac{\sinh\left(\lambda_r\right) - \sin\left(\lambda_r\right)}{\cosh\left(\lambda_r\right) - \cos\left(\lambda_r\right)} \tag{25}$$

where C_r is the mass normalization constant for the rth mode and λ_r are the eigenvalues associated to the analytical solution obtained by the following characteristic equation

$$\cos\left(\lambda_r\right)\cosh\left(\lambda_r\right) - 1 = 0 \tag{26}$$

Alternatively, Ganesan & Engels (1992) propose enrichment functions based on the same analytical solution but in the form presented by Gartner & Olgac (1982) given by

$$F_r = \frac{1}{\sqrt{\rho A L_e}}\left[\cos\left(\lambda_r\xi\right) - \frac{1 + \left(-1\right)^r e^{-\lambda_r}}{1 - \left(-1\right)^r e^{-\lambda_r}}\sin\left(\lambda_r\xi\right) - \frac{e^{-\lambda_r\xi} - \left(-1\right)^r e^{-\lambda_r\left(1-\xi\right)}}{1 - \left(-1\right)^r e^{-\lambda_r}}\right] \tag{27}$$

where λ_r are the eigenvalues obtained by solving the equation

$$\cos\left(\lambda_r\right)-\frac{2e^{-\lambda_r}}{1+e^{-2\lambda_r}}=0 \tag{28}$$

Ganesan & Engels (1992) also propose trigonometric enrichment functions in the following form:

$$F_r=\cos\left[\left(r-1\right)\pi\xi\right]-\cos\left[\left(r+1\right)\pi\xi\right] \tag{29}$$

The Composite Element Method (CEM), proposed by Zeng (1998b), uses enrichment functions given by:

$$F_r=\sin\left(\lambda_r\xi\right)-\sinh\left(\lambda_r\xi\right)-\frac{\sin\lambda_r-\sinh\lambda_r}{\cos\lambda_r-\cosh\lambda_r}\left[\cos\left(\lambda_r\xi\right)-\cosh\left(\lambda_r\xi\right)\right] \tag{30}$$

corresponding to the clamped-clamped beam free vibration solution where λ_r are the eigenvalues obtained by the solution of Eq. (26).
Leung & Chan (1998) propose two types of enrichment functions based on the Fourier series: the cosine version

$$F_r=1-\cos\left(r\pi\xi\right) \tag{31}$$

and the sine version

$$F_r=\xi\left(1-\xi\right)\sin\left(r\pi\xi\right)\,. \tag{32}$$

The cosine version is the simplest but is not recommended when modeling a free of shear forces structure with only one element. Leung & Chan (1998) also note that the cosine version fails to predict the clamped-hinged and clamped-clamped modes of beams.
It is noteworthy that all these functions and their first derivatives vanish at element nodes. Again this feature allows the introduction of boundary conditions following the standard finite element procedure.

4. Generalized finite element method

The Generalized Finite Element Method (GFEM) is a Galerkin method whose main goal is the construction of a finite dimensional subspace of approximating functions using local knowledge about the solution that ensures accurate local and global results. The GFEM local enrichment in the approximation subspace is incorporated by the partition of unity approach.

4.1 Partition on unity

The Partition of Unity Method is defined as follows.
Let $u\in H^1\left(\Omega\right)$ be the function to be approximated and $\left\{\Omega_i\right\}$ be an open cover of domain Ω (Fig. 3) satisfying an overlap condition:

$$\exists M_S\in\mathbf{N}\quad\text{so that}\quad\forall x\in\Omega\quad card\left\{\,i\middle|x\in\Omega_i\right\}\le M_S\,. \tag{33}$$

A partition of unity subordinate to the cover $\left\{\Omega_i\right\}$ is the set of functions $\left\{\eta_i\right\}$ satisfying the conditions:

$$\text{supp}\,(\eta_i) = \{\, x \in \Omega \; | \eta_i(x) \neq 0 \} \subset [\Omega_i], \quad \forall i \tag{34}$$

$$\sum_i \eta_i \; \equiv 1 \;\text{ on }\; \Omega \tag{35}$$

where $\text{supp}\,(\eta_i)$ denotes the support of definition of the function η_i and $[\Omega_i]$ is the closure of the patch Ω_i.

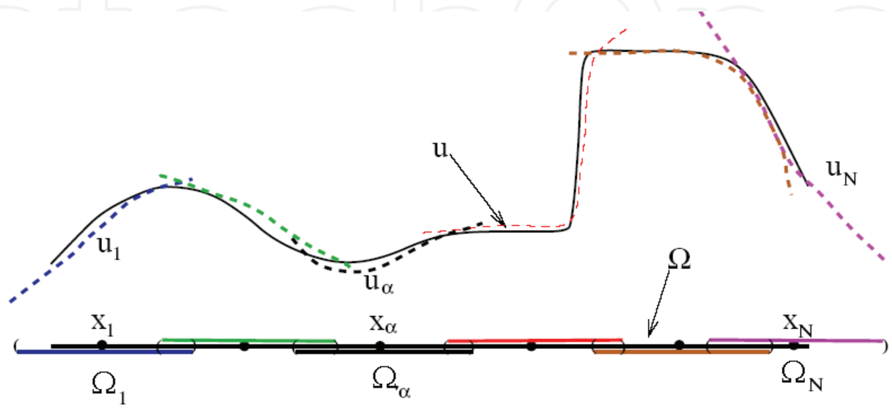

Fig. 3. Open cover $\{\Omega_i\}$ of domain Ω (Duarte et al., 2000)

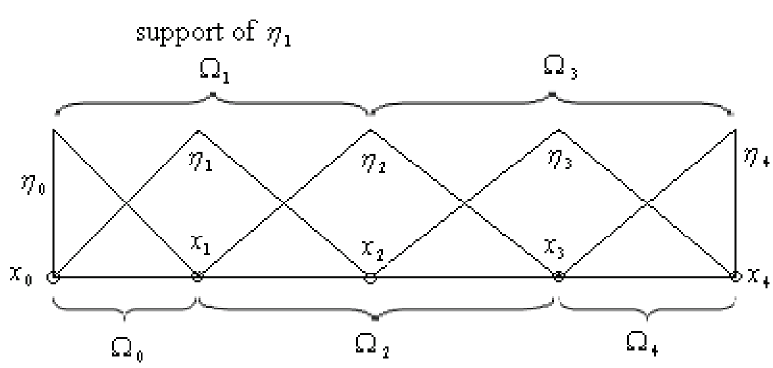

Fig. 4. Patchs and partition of unity set for one-dimensional GFEM finite element mesh

The partition of unity set $\{\eta_i\}$ allows to obtain an enriched set of approximating functions. Let $S_i \subset H^1(\Omega_i \cap \Omega)$ be a set of functions that locally well represents u:

$$S_i = \{s_i^j\}_{j=1}^{m} \tag{36}$$

Then the enriched set is formed by multiplying each partition of unity function η_i by the corresponding s_i^j, i.e.,

$$S := \sum_i \eta_i \; S_i = \left\{ \sum_i \eta_i \; s_i^j \;\; | s_i^j \in S_i \right\} \subset H^1(\Omega) \tag{37}$$

Accordingly, the function u can be approximated by the enriched set as:

$$u_h(x) = \sum_i \sum_{s_i^j \in S_i} \eta_i s_i^j(x) \; a_{ij} \tag{38}$$

where a_{ij} are the degrees of freedom.
The proposed C^0 and C^1 generalized elements for free vibration analysis of framed structures are described below. The *h*, *p* and adaptive refinements of these elements are discussed.
In the proposed GFEM, the cover $\{\Omega_i\}$ corresponds to the finite element mesh and each patch Ω_i corresponds to the sub domain of Ω formed by the union of elements that contain the node x_i (Fig. 4).

4.2 Generalized C^0 elements

The generalized C^0 elements use the classical linear FEM shape functions as the partition of unity, i.e.:

$$\eta_i = \begin{cases} 1 + \dfrac{x - x_i}{x_i - x_{i-1}} & if\ x \in (x_{i-1}, x_i) \\ 1 - \dfrac{x - x_i}{x_{i+1} - x_i} & if\ x \in (x_i, x_{i+1}) \end{cases} \tag{39}$$

in the patch $\Omega_i = (x_{i-1}, x_{i+1})$.
The proposed local approximation space in the patch $\Omega_i = (x_{i-1}, x_{i+1})$ takes the form:

$$S_i = span\{\ 1 \quad \gamma_{1j} \quad \gamma_{2j} \quad \phi_{1j} \quad \phi_{2j} \quad \ldots\},\ j = 1, 2, \ldots, n_l \tag{40}$$

$$\gamma_{1j} = \begin{cases} 0 \ \ if \quad x \in (x_{i-1}, x_i) \\ \sin\left[\beta_{Rj}(x - x_i)\right] \ \ if \quad x \in (x_i, x_{i+1}) \end{cases} \tag{41}$$

$$\gamma_{2j} = \begin{cases} \sin\left[\beta_{Lj}(x - x_i)\right] \ \ if \quad x \in (x_{i-1}, x_i) \\ 0 \ \ if \quad x \in (x_i, x_{i+1}) \end{cases} \tag{42}$$

$$\phi_{1j} = \begin{cases} 0 \ \ if \quad x \in (x_{i-1}, x_i) \\ \cos\left[\beta_{Rj}(x - x_i)\right] - 1 \ \ if \quad x \in (x_i, x_{i+1}) \end{cases} \tag{43}$$

$$\phi_{2j} = \begin{cases} \cos\left[\beta_{Lj}(x - x_i)\right] - 1 \ \ if \quad x \in (x_{i-1}, x_i) \\ 0 \ \ if \quad x \in (x_i, x_{i+1}) \end{cases} \tag{44}$$

$$\beta_{Rj} = \sqrt{\frac{\rho_R}{E_R}}\mu_j \tag{45}$$

$$\beta_{Lj} = \sqrt{\frac{\rho_L}{E_L}}\mu_j \tag{46}$$

where E_R and ρ_R are the Young modulus and specific mass on sub domain (x_i, x_{i+1}), E_L and ρ_L are the Young modulus and specific mass on sub domain (x_{i-1}, x_i), and μ_j is a frequency related to the enrichment level *j*.

The enriched functions, so proposed, vanish at element nodes, which allows the imposition of boundary conditions in the same fashion of the finite element procedure.

This C^0 element can be applied to the free vibration analysis of shafts, bars and trusses. Different frequencies μ_j produce different enriched elements. The increase in the number of elements in the mesh with only one level of enrichment (j = 1) and a fixed parameter $\beta_1 = \beta_{R1} = \beta_{L1}$, $\beta_1 = \pi$ for example, produces an h refinement. Otherwise the increase in the number of levels of enrichment, with a different parameter $\beta_j = \beta_{Rj} = \beta_{Lj}$ each, $\beta_j = j\pi$ for example, produces a hierarchical p refinement. Another possible refinement in the proposed GFEM is the adaptive one, which is presented below.

The adaptive GFEM is an iterative approach presented first by Arndt et al. (2010) whose main goal is to increase the accuracy of the frequency (eigenvalue) related to a chosen vibration mode with order denoted by "target order". The flowchart with blocks A to H presented in Fig. 5 represents the adaptive process.

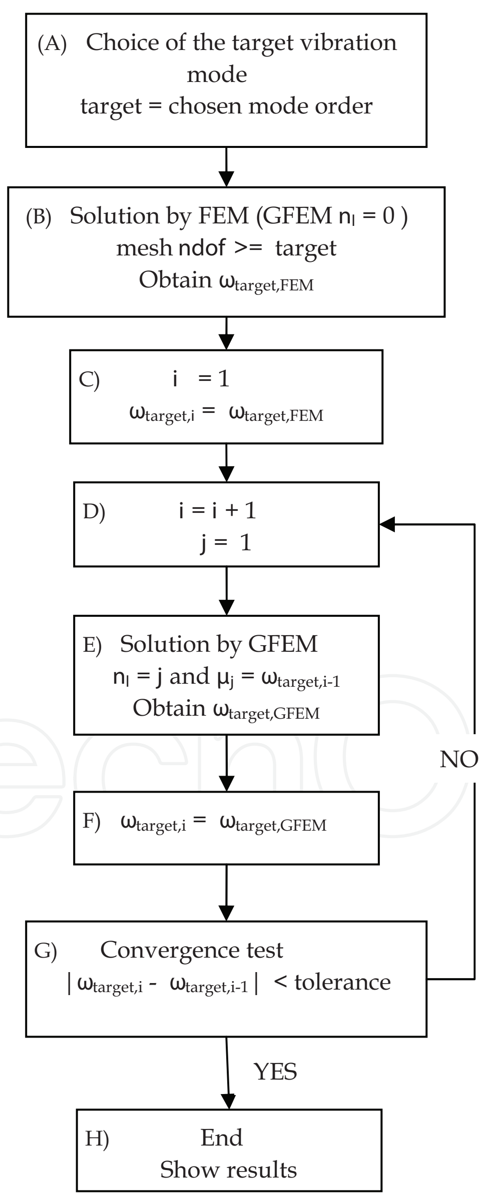

Fig. 5. Flowchart of the adaptive GFEM

In this flowchart, ω_{target} corresponds to the frequency related to the target mode. The first step of the adaptive GFEM process (blocks A to C) consists in obtaining an approximation of the target frequency by the standard FEM (GFEM with n_l = 0) with a coarse mesh. The finite element mesh used in the analysis has to be as coarse as necessary to capture a first approximation of the target frequency. The subsequent steps (blocks D to G) consist in applying the GFEM with only one enrichment level (n_l = 1) to the same finite element mesh assuming the frequency μ_j (j = 1, blocks D and E) of the enrichment functions (Eqs. 41-46) as the target frequency obtained in the last step. Thus, no mesh refinement is necessary along the iterative process.

Both the standard FEM and the adaptive GFEM allow as many frequencies as the total number of degrees of freedom to be obtained. However, in the latter, only the precision of the target frequency is effectively improved by the iterative process. The other frequencies present errors similar to those obtained by the standard FEM with the same mesh. In order to improve the precision of another frequency, it is necessary to perform a new adaptive GFEM analysis, taking this new one as the target frequency.

4.3 Generalized C¹ elements

The generalized C¹ elements also use the classical linear FEM form functions as partition of unity (Eq. (39)). The proposed local approximation space in the patch $\Omega_i = (x_{i-1}, x_{i+1})$ takes the form:

$$S_i = span\left\{ \varphi_1 \quad \varphi_2 \quad \gamma_{1j} \quad \gamma_{2j} \quad \dots \right\}, \quad j = 1, 2, \dots, n_l \tag{47}$$

$$\varphi_1 = \begin{cases} 3\dfrac{x - x_{i-1}}{x_i - x_{i-1}} - 2\left(\dfrac{x - x_{i-1}}{x_i - x_{i-1}}\right)^2 & if \quad x \in (x_{i-1}, x_i) \\ 1 + \dfrac{x - x_i}{x_{i+1} - x_i} - 2\left(\dfrac{x - x_i}{x_{i+1} - x_i}\right)^2 & if \quad x \in (x_i, x_{i+1}) \end{cases} \tag{48}$$

$$\varphi_2 = \begin{cases} \left[\left(\dfrac{x - x_{i-1}}{x_i - x_{i-1}}\right)^2 - \dfrac{x - x_{i-1}}{x_i - x_{i-1}}\right](x_i - x_{i-1}) & if \quad x \in (x_{i-1}, x_i) \\ \left[\dfrac{x - x_i}{x_{i+1} - x_i} - \left(\dfrac{x - x_i}{x_{i+1} - x_i}\right)^2\right](x_{i+1} - x_i) & if \quad x \in (x_i, x_{i+1}) \end{cases} \tag{49}$$

$$\gamma_{1j} = \begin{cases} \cos(\lambda_j z_1) - \dfrac{1 + (-1)^j e^{-\lambda_j}}{1 - (-1)^j e^{-\lambda_j}} \sin(\lambda_j z_1) - \dfrac{e^{-\lambda_j z_1} - (-1)^j e^{-\lambda_j (1 - z_1)}}{1 - (-1)^j e^{-\lambda_j}} & if \quad x \in (x_{i-1}, x_i) \\ 0 \quad if \quad x \in (x_i, x_{i+1}) \end{cases}$$
$$z_1 = \frac{x - x_{i-1}}{x_i - x_{i-1}} \tag{50}$$

$$\gamma_{2j} = \begin{cases} 0 \quad if \quad x \in (x_{i-1}, x_i) \\ \cos(\lambda_j z_2) - \dfrac{1+(-1)^j e^{-\lambda_j}}{1-(-1)^j e^{-\lambda_j}} \sin(\lambda_j z_2) - \dfrac{e^{-\lambda_j z_2} - (-1)^j e^{-\lambda_j (1-z_2)}}{1-(-1)^j e^{-\lambda_j}} \quad if \quad x \in (x_i, x_{i+1}) \end{cases} \tag{51}$$

$$z_2 = \frac{x - x_i}{x_{i+1} - x_i}$$

where λ_j are the eigenvalues obtained by the solution of Eq. (28).

Such partition of unity functions and local approximation space produce the cubic FEM approximation space enriched by functions that represent the local behavior of the differential equation solution. The enriched functions and their first derivatives vanish at element nodes. Hence, the imposition of boundary conditions follows the finite element procedure. This C^1 element is suited to apply to the free vibration analysis of Euler-Bernoulli beams.

Again the increase in the number of elements in the mesh with only one level of enrichment (j = 1) and a fixed eigenvalue λ_1 produces the *h* refinement of GFEM. Otherwise the increase in the number of levels of enrichment, each of one with a different frequency λ_j, produces a hierarchical *p* refinement. An adaptive GFEM refinement for free vibration analysis of Euler-Bernoulli beams is straight forward, as can be easily seen. However it will not be discussed here.

5. Applications

Numerical solutions for two bars, a beam and a truss are given below to illustrate the application of the GFEM. To check the efficiency of this method the results are compared to those obtained by the *h* and *p*-versions of FEM and the *c*-version of CEM.

The number of degrees of freedom (ndof) considered in each analysis is the total number of effective degrees of freedom after introduction of boundary conditions. As an intrinsic imposition of the adaptive method, each target frequency is obtained by a new iterative analysis. The mesh used in each adaptive analysis is the coarser one, that is, just as coarse as necessary to capture a first approximation of the target frequency.

5.1 Uniform fixed-free bar

The axial free vibration of a fixed-free bar (Fig. 6) with length *L*, elasticity modulus *E*, mass density ρ and uniform cross section area *A*, has exact natural frequencies (ω_r) given by (Craig, 1981):

$$\omega_r = \frac{(2r-1)\pi}{2L}\sqrt{\frac{E}{\rho}} \quad , \ r = 1,2,\ldots . \tag{52}$$

In order to compare the exact solution with the approximated ones, in this example it is used a non-dimensional eigenvalue χ_r given by:

$$\chi_r = \frac{\rho L^2 \omega_r{}^2}{E} . \tag{53}$$

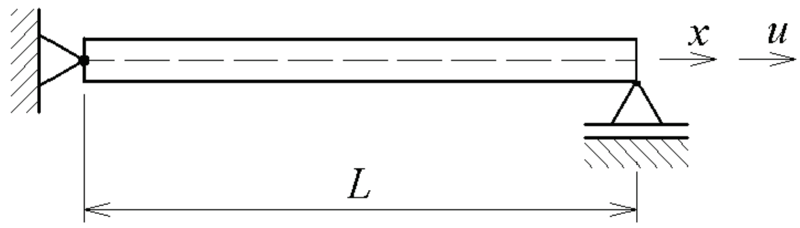

Fig. 6. Uniform fixed-free bar

a) *h* refinement

First the proposed problem is analyzed by a series of *h* refinements of FEM (linear and cubic), CEM and GFEM (C^0 element). A uniform mesh is used in all methods. Only one enrichment function is used in each element of the *h*-version of CEM. One level of enrichment (n_l = 1) with $\beta_1 = \pi$ is used in the *h*-version of GFEM. The evolution of relative error of the *h* refinements for the six earliest eigenvalues in logarithmic scale is presented in Figs. 7-9.

The results show that the *h*-version of GFEM exhibits greater convergence rates than the *h* refinements of FEM and CEM for all analyzed eigenvalues.

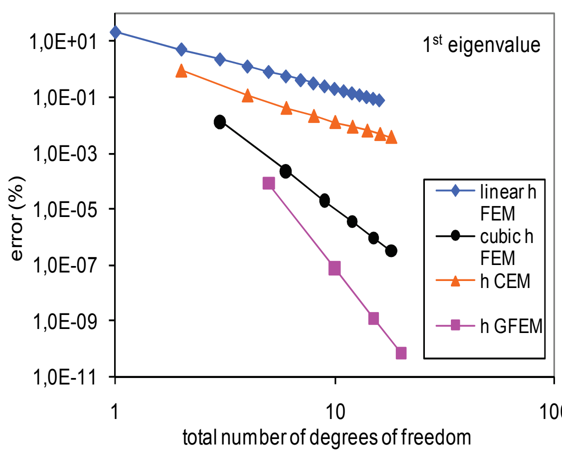

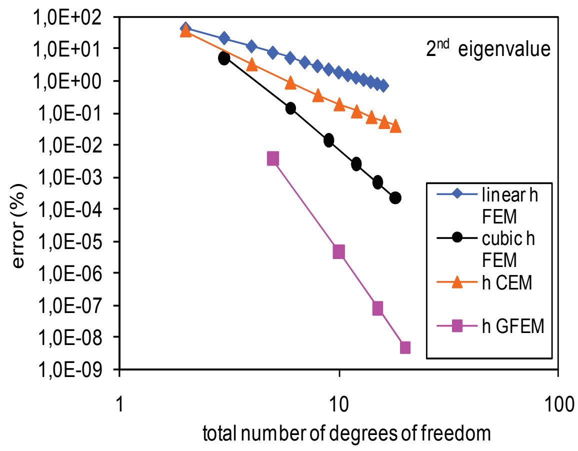

Fig. 7. Relative error (%) for the 1st and 2nd fixed-free bar eigenvalues – *h* refinements

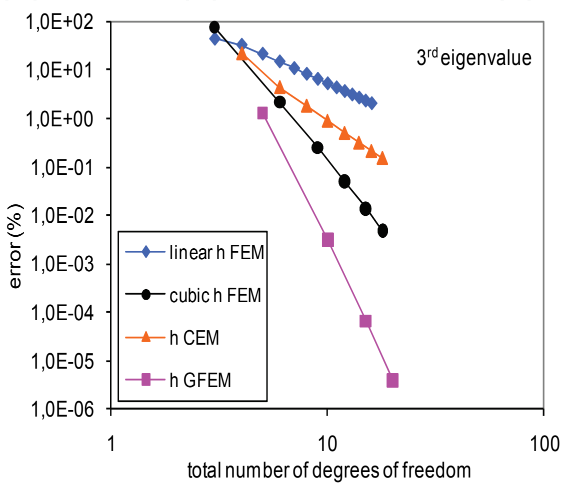

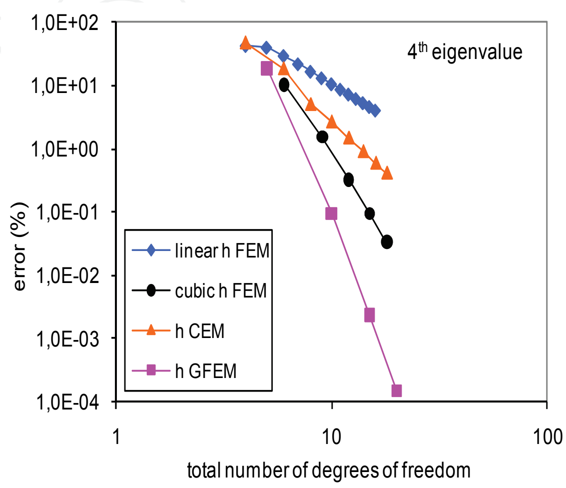

Fig. 8. Relative error (%) for the 3rd and 4th fixed-free bar eigenvalues - *h* refinements

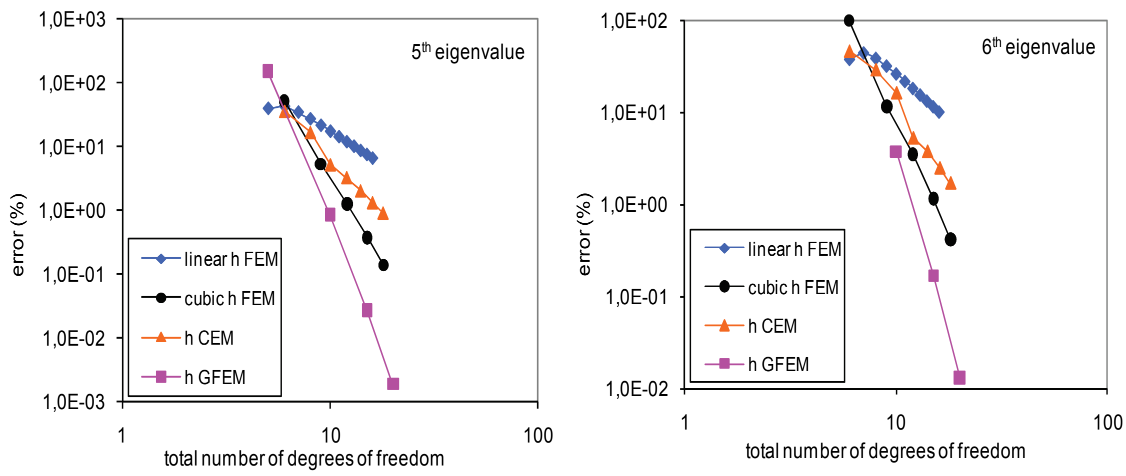

Fig. 9. Relative error (%) for the 5th and 6th fixed-free bar eigenvalues - *h* refinements

b) *p* refinement

The *p* refinement of GFEM is now compared to the hierarchical *p*-version of FEM and the *c*-version of CEM. The *p*-version of GFEM consists in a progressive increase of levels of enrichment with parameter $\beta_j = j\pi$.

The evolution of relative error of the *p* refinements for the six earliest eigenvalues in logarithmic scale is presented in Figs. 10-12.

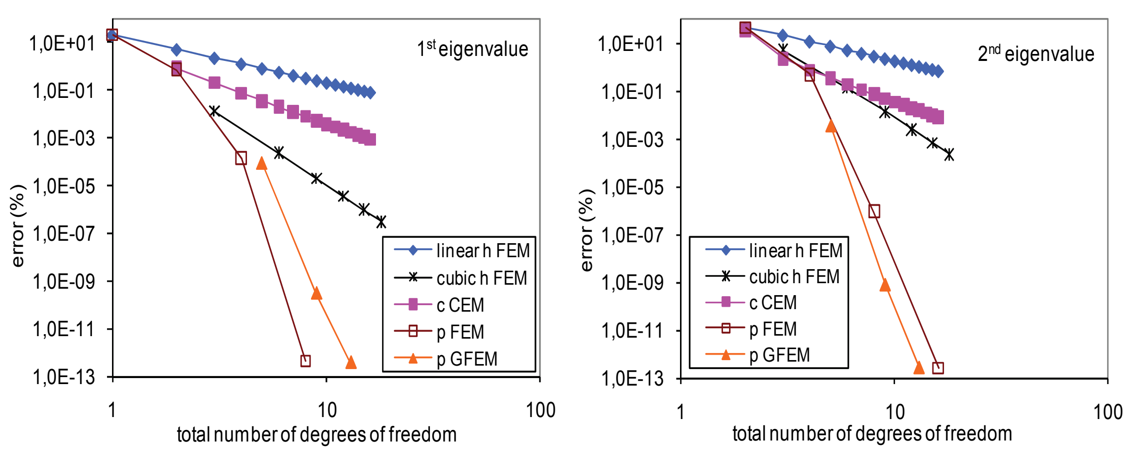

Fig. 10. Relative error (%) for the 1st and 2nd fixed-free bar eigenvalues - *p* refinements

The fixed-free bar results show that the *p*-version of GFEM presents greater convergence rates than the *h* refinements of FEM and the *c*-version of CEM. The hierarchical *p* refinement of FEM only overcomes the results obtained by *p*-version of GFEM for the first eigenvalue. For the other eigenvalues the GFEM presents more precise results and greater convergence rates.

c) adaptive refinement

Four different adaptive GFEM analyses are performed in order to obtain the first four frequencies. The behavior of the relative error in each analysis is presented in Fig. 13.

In order to capture an initial approximation of the target vibration frequency, for the first frequency, the finite element mesh must have at least one bar element (one effective degree of freedom), for the second frequency, it must have at least two bar elements (two effective degrees of freedom), and so on.

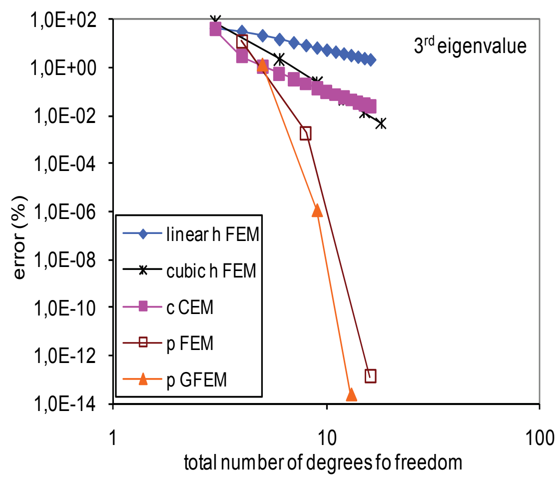

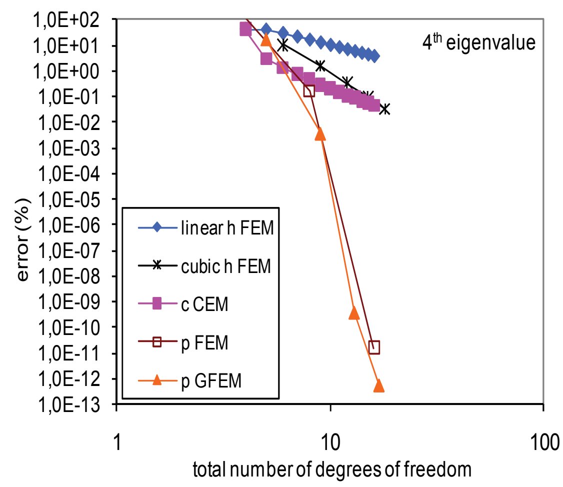

Fig. 11. Relative error (%) for the 3rd and 4th fixed-free bar eigenvalues - p refinements

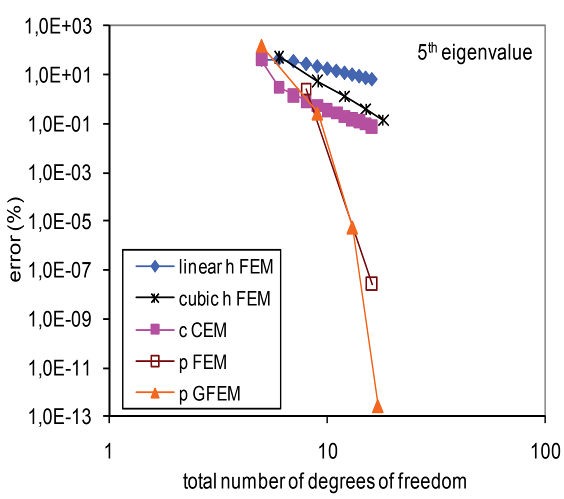

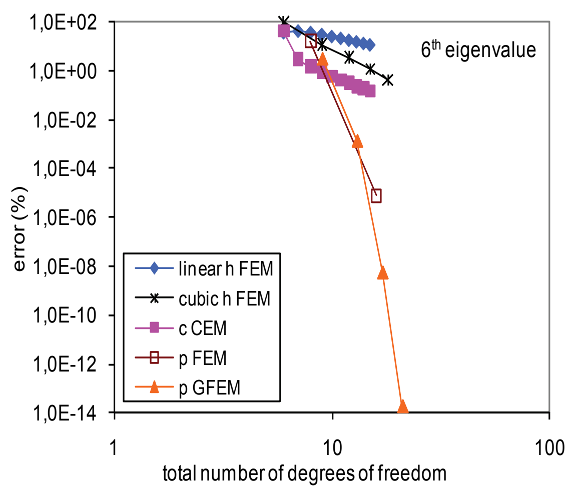

Fig. 12. Relative error (%) for the 5th and 6th fixed-free bar eigenvalues - p refinements

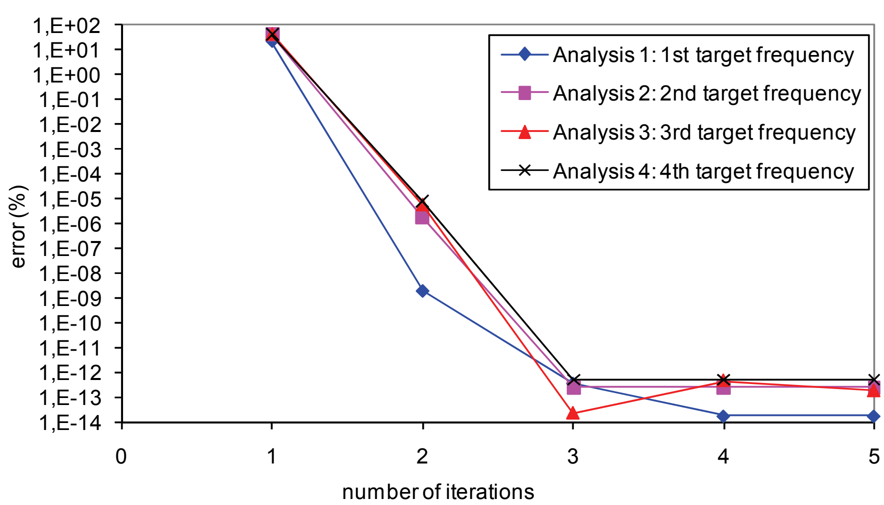

Fig. 13. Error in the adaptive GFEM analyses of fixed-free uniform bar

Table 1 presents the relative errors obtained by the numerical methods. The linear FEM solution is obtained with 100 elements, that is, 100 effective degrees of freedom (dof). The cubic FEM solution is obtained with 20 elements, that is, 60 effective degrees of freedom. The CEM solution is obtained with one element and 15 enrichment functions corresponding to one nodal degree of freedom and 15 field degrees of freedom resulting in 16 effective degrees of freedom. The hierarchical p FEM solution is obtained with a 17-node element corresponding to 16 effective degrees of freedom. The analyses by the adaptive GFEM have no more than 20 degrees of freedom in each iteration. For example, the fourth frequency is obtained taking 4 degrees of freedom in the first iteration and 20 degrees of freedom in the two subsequent ones.

Eigenvalue	linear h FEM (100e) ndof = 100	cubic h FEM (20e) ndof = 60	p FEM (1e 17n) ndof = 16	c CEM (1e 15c) ndof =16	Adaptive GFEM (after 3 iterations)	
	error (%)	error (%)	error (%)	error (%)	error (%)	ndof in iterations
1	2,056 e-3	8,564 e-10	3,780 e-13	8,936 e-4	3,780 e-13	1x 1 dof + 2x 5 dof
2	1,851 e-2	1,694 e-7	2,560 e-13	8,188 e-3	2,560 e-13	1x 2 dof + 2x 10 dof
3	5,141 e-2	3,619 e-6	1,382 e-13	2,299 e-2	2,304 e-14	1x 3 dof + 2x 15 dof
4	1,008 e-1	2,711 e-5	1,602 e-11	4,579 e-2	5,289 e-13	1x 4 dof + 2x 20 dof

Table 1. Results to free vibration of uniform fixed-free bar

The adaptive process converges rapidly, requiring three iterations in order to achieve each target frequency with precision of the 10^{-13} order. For the uniform fixed-free bar, one notes that the adaptive GFEM reaches greater precision than the h versions of FEM and the c-version of CEM. The p-version of FEM is as precise as the adaptive GFEM only for the first two eigenvalues. After this, the precision of the adaptive GFEM prevails among the others. For the sake of comparison, the standard FEM software Ansys© employing 410 truss elements (LINK8) reaches the same precision for the first four frequencies.

5.2 Fixed-fixed bar with sinusoidal variation of cross section area

In order to analyze the efficiency of the adaptive GFEM for non-uniform bars, the longitudinal free vibration of a fixed-fixed bar with sinusoidal variation of cross section area, length L, elasticity modulus E and mass density ρ is analyzed. The boundary conditions are $\bar{u}(0,t)=0$ and $\bar{u}(L,t)=0$, and the cross section area varies as

$$A(x) = A_0 \sin^2\left(\frac{x}{L}+1\right) \tag{54}$$

where A_0 is a reference cross section area.

Kumar & Sujith (1997) presented exact analytical solutions for longitudinal free vibration of bars with sinusoidal and polynomial area variations.

This problem is analyzed by the h and p versions of FEM and the adaptive GFEM. Six adaptive analyses are performed in order to obtain each of the first six frequencies. The behavior of the relative error of the target frequency in each analysis is presented in Fig. 14.

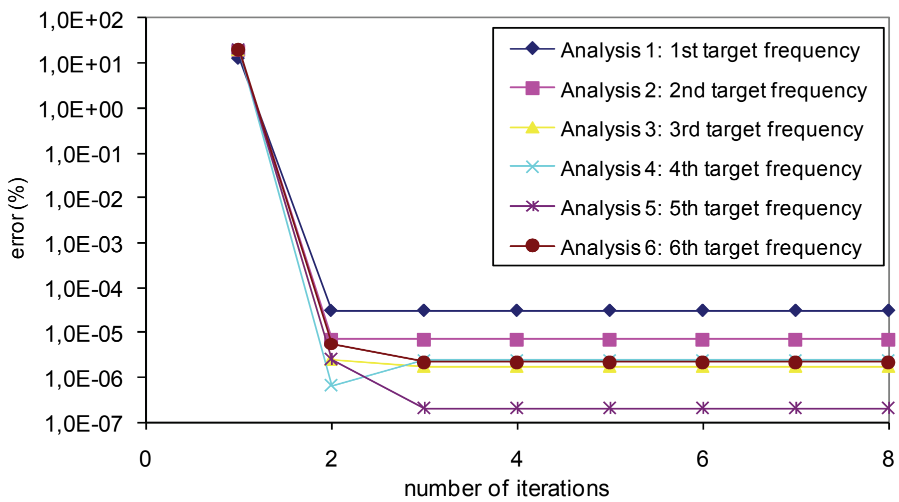

Fig. 14. Error in the adaptive GFEM analyses of fixed-fixed non-uniform bar

Table 2 shows the first six non-dimensional eigenvalues ($\beta_r = \omega_r L\sqrt{\rho/E}$) and their relative errors obtained by these methods. The linear h FEM solution is obtained with 100 elements, that is, 99 effective degrees of freedom after introduction of boundary conditions. The cubic h FEM solution is obtained with 12 cubic elements, that is, 35 effective degrees of freedom. The p FEM solution is obtained with one hierarchical 33-node element, that is, 31 effective degrees of freedom. The analyses by the adaptive GFEM have maximum number of degrees of freedom in each iteration ranging from 9 to 34.

r	Analytical solution (Kumar & Sujith, 1997)	linear h FEM (100e) ndof = 99	cubic h FEM (12e) ndof = 35	hierarchical p FEM (1e 33n) ndof = 31	Adaptive GFEM (after 3 iterations)	
	χ_r	error (%)	error (%)	error (%)	error (%)	ndof in iterations
1	2,978189	4,737 e-3	2,577 e-5	2,998 e-5	2,997 e-5	1x 1 dof + 2x 9 dof
2	6,203097	1,699 e-2	1,901 e-4	6,774 e-6	6,871 e-6	1x 2 dof + 2x 14 dof
3	9,371576	3,753 e-2	3,065 e-4	1,643 e-6	1,731 e-6	1x 3 dof + 2x 19 dof
4	12,526519	6,632 e-2	7,312 e-4	2,498 e-6	2,441 e-6	1x 4 dof + 2x 24 dof
5	15,676100	1,033 e-1	2,332 e-3	2,407 e-7	2,044 e-7	1x 5 dof + 2x 29 dof
6	18,823011	1,486 e-1	6,787 e-3	2,163 e-6	2,187 e-6	1x 6 dof + 2x 34 dof

Table 2. Results to free vibration of non-uniform fixed-fixed bar

The adaptive GFEM exhibits more accuracy than the h-versions of FEM with even less degrees of freedom. The precision reached for all calculated frequencies by the adaptive process is similar to the p-version of FEM with 31 degrees of freedom. The errors are greater than those from the uniform bars because the analytical vibration modes of non-uniform bars cannot be exactly represented by the trigonometric functions used as enrichment functions; however, the precision is acceptable for engineering applications. Each analysis by the adaptive GFEM is able to refine the target frequency until the exhaustion of the approximation capacity of the enriched subspace.

5.3 Uniform clamped-free beam

The free vibration of an uniform clamped-free beam (Fig. 15) in lateral motion, with length L, second moment of area I, elasticity modulus E, mass density ρ and cross section area A, is analyzed in order to demonstrate the application of the proposed method. The analytical natural frequencies (ω_r) are the roots of the equation:

$$\cos(\kappa_r L)\cosh(\kappa_r L)+1=0\,,\ r=1,2,\ldots \tag{55}$$

$$\kappa_r=\sqrt[4]{\frac{\omega_r^{\,2}\rho A}{EI}} \tag{56}$$

To check the efficiency of the proposed generalized C^1 element the results are compared to those obtained by the h and p versions of FEM and by the c refinement of CEM. The eigenvalue $\chi_r=\kappa_r.L$ is used to compare the analytical solution with the approximated ones.

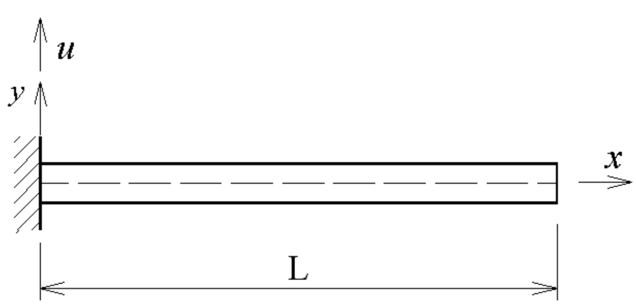

Fig. 15. Uniform clamped-free beam

a) *h* refinement

First this problem is analyzed by the h refinement of FEM, CEM and GFEM. A uniform mesh is used in all methods. Only one enrichment function is used in each element of the h-version of CEM. One level of enrichment (n_l = 1) is used in the h-version of GFEM.
The evolution of the relative error of the h refinements for the four earliest eigenvalues in logarithmic scale is presented in Figs. 16 and 17.

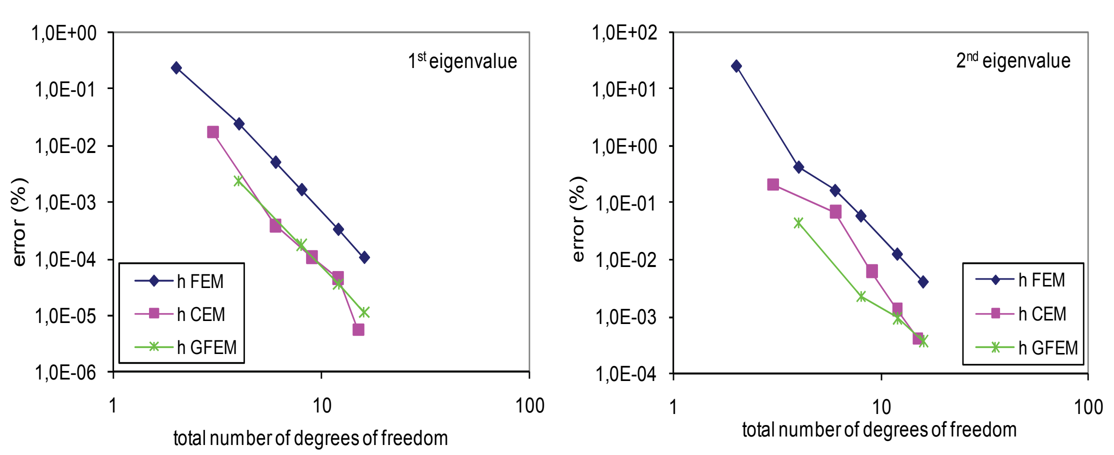

Fig. 16. Relative error (%) for the 1st and 2nd clamped-free beam eigenvalues – h refinements

The results show that the h-version of GFEM presents greater convergence rates than the h refinement of FEM. The results of h-version of CEM for the first two eigenvalues resemble those obtained by the *h*-version of GFEM. However the results of *h*-version of GFEM for higher eigenvalues are more accurate.

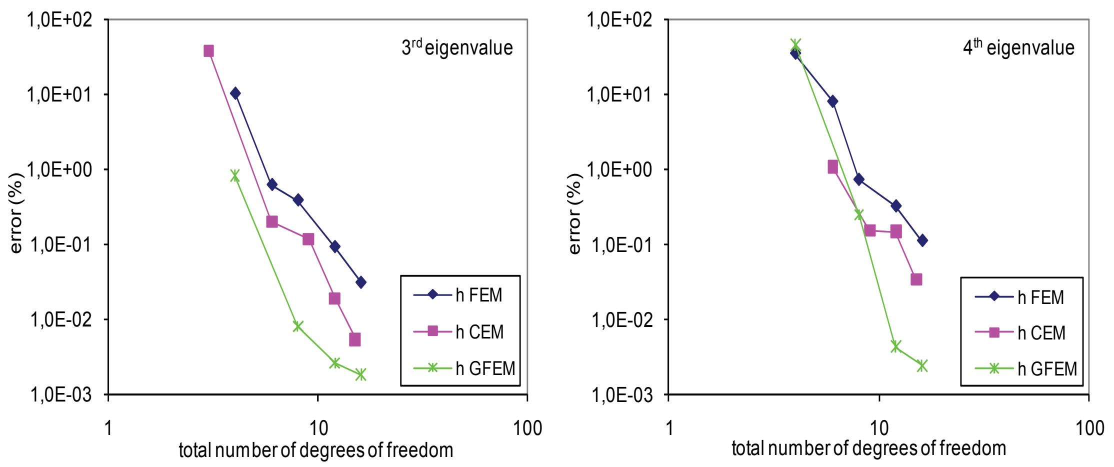

Fig. 17. Relative error (%) for the 3rd and 4th clamped-free beam eigenvalues – *h* refinements

b) *p* refinement

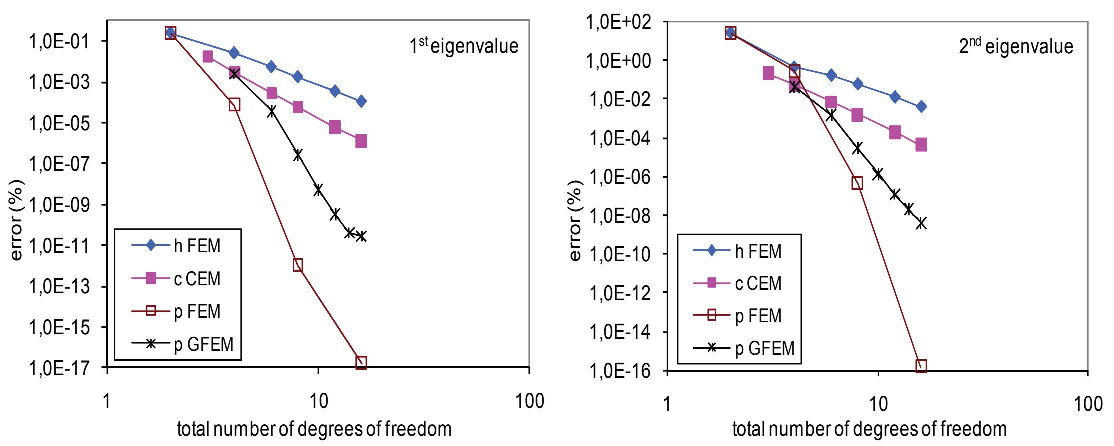

Fig. 18. Relative error (%) for the 1st and 2nd clamped-free beam eigenvalues – *p* refinements

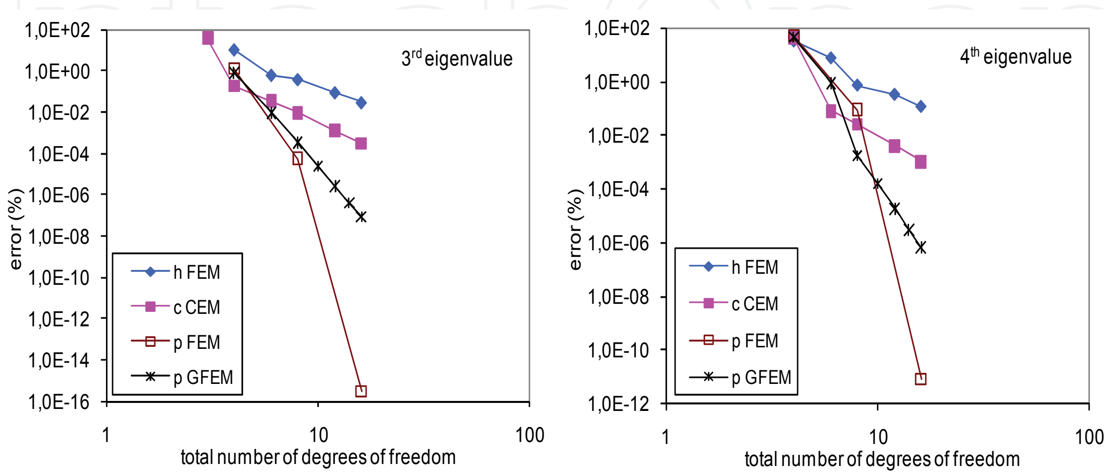

Fig. 19. Relative error (%) for the 3rd and 4th clamped-free beam eigenvalues – *p* refinements

The p refinement of GFEM is now compared to the hierarchical p-version of FEM and the c-version of CEM. The p-version of GFEM consists in a progressive increase of levels of enrichment. The relative error evolution of the p refinements for the first eight eigenvalues in logarithmic scale is presented in Figs. 18-21.
The results of the p-version of GFEM converge more rapidly than those obtained by the h-version of FEM and the c-version of CEM. The hierarchical p-version of FEM overcomes the precision and convergence rates obtained by the p-version of GFEM for the first six eigenvalues. However the p-version of GFEM is more precise for higher eigenvalues.

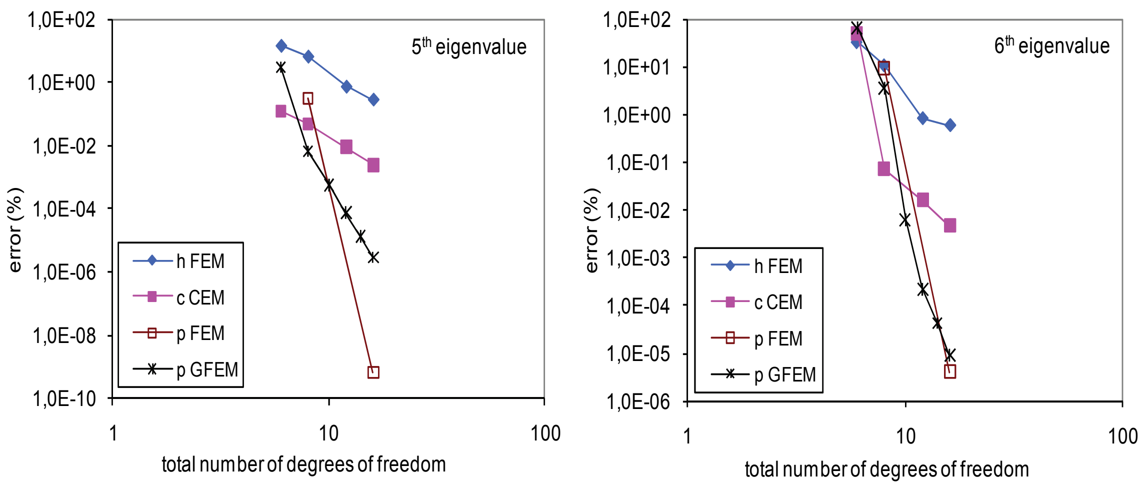

Fig. 20. Relative error (%) for the 5th and 6th clamped-free beam eigenvalues – p refinements

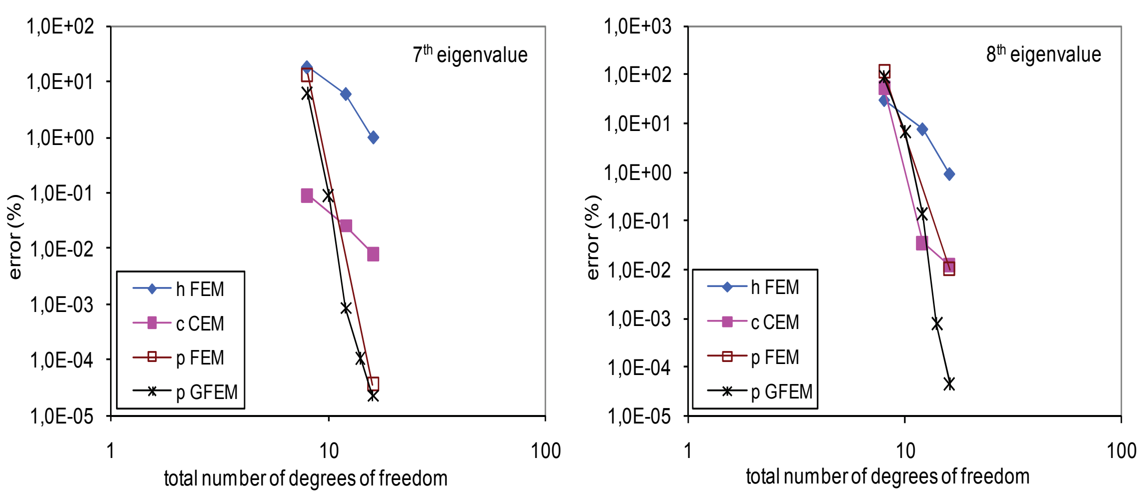

Fig. 21. Relative error (%) for the 7th and 8th clamped-free beam eigenvalues – p refinements

5.4 Seven bar truss

The free axial vibration of a truss formed by seven straight bars is analyzed to illustrate the application of the adaptive GFEM in structures formed by bars. This problem is proposed by Zeng (1998a) in order to check the CEM. The geometry of the truss is presented in Fig. 22. All bars in the truss have cross section area A = 0,001 m^2, mass density ρ = 8000 kg m^{-3} and elasticity modulus E = 2,1 10^{11} N m^{-2}.

All analyses use seven element mesh, the minimum number of C^0 type elements necessary to represent the truss geometry. The linear FEM, the *c*-version of CEM and the *h*-version of GFEM with $n_l = 1$ and $\beta_1 = \pi$ are applied. Six analyses by the adaptive GFEM are performed in order to improve the accuracy of each of the first six natural frequencies. The frequencies obtained by each analysis are presented in Table 3.

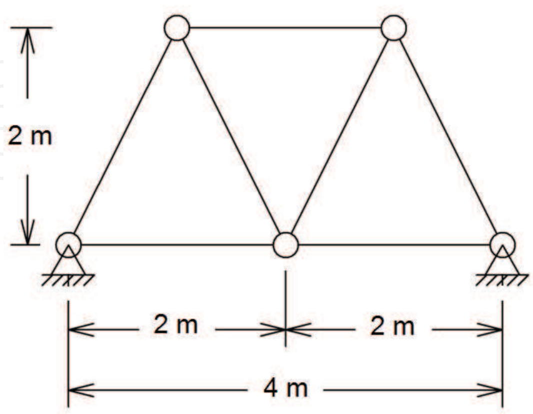

Fig. 22. Seven bar truss

	FEM (7e) ndof = 6	CEM (7e 1c) ndof = 13	CEM (7e 2c) ndof = 20	CEM (7e 5c) ndof = 41	*h* GFEM (7e) $n_l = 1$, $\beta_1 = \pi$ ndof = 34	Adaptive GFEM (7e 3i) 1x 6 dof + 2x 34 dof
i	ω_i (rad/s)	ω_i (rad/s)	ω_i (rad/s)	ω_i (rad/s)	ω_i (rad/s)	ω_i (rad/s)
1	1683,521413	1648,516148	1648,258910	1647,811939	1647,785439	1647,784428
2	1776,278483	1741,661466	1741,319206	1740,868779	1740,840343	1740,839797
3	3341,375203	3119,123132	3113,835167	3111,525066	3111,326191	3111,322715
4	5174,353866	4600,595156	4567,688849	4562,562379	4561,819768	4561,817307
5	5678,184561	4870,575795	4829,702095	4824,125665	4823,253509	4823,248678
6	8315,400602	7380,832845	7379,960217	7379,515018	7379,482416	7379,482322

Table 3. Results to free vibration of seven bar truss

The FEM solution is obtained with seven linear elements, that is, six effective degrees of freedom after introduction of boundary conditions. The *c*-version of the CEM solution is obtained with seven elements and one, two and five enrichment functions corresponding to six nodal degrees of freedom and seven, 14 and 35 field degrees of freedom respectively. All analyses by the adaptive GFEM have six degrees of freedom in the first iteration and 34 degrees of freedom in the following two.

This special case is not well suited to the *h*-version of FEM since it demands the adoption of restraints at each internal bar node in order to avoid modeling instability. The FEM analysis of this truss can be improved by applying bar elements of higher order (*p*-version) or beam elements. The results show that both the *c*-version of CEM and the adaptive GFEM converges to the same frequencies.

6. Conclusion

The main contribution of the present study consists in formulating and investigating the performance of the Generalized Finite Element Method (GFEM) for vibration analysis of framed structures. The proposed generalized C^0 and C^1 elements allow to apply boundary conditions as in the standard finite element procedure. In some of the recently proposed methods such as the modified CEM (Lu & Law, 2007), it is necessary to change the set of shape functions depending on the boundary conditions of the problem. In others, like the Partition of Unity used by De Bel et al. (2005) and Hazard & Bouillard (2007), the boundary conditions are applied under a penalty approach. In addition the GFEM enrichment functions require less effort to be obtained than the FEM shape functions in a hierarchical *p* refinement.

The GFEM results were compared with those obtained by the *h* and *p* versions of FEM and the *c*-version of CEM. The *h*-version of GFEM for C^0 elements exhibits more accuracy than *h* refinements of FEM and CEM. The C^1 *h*-version of GFEM presents more accurate results than *h*-version of FEM for all beam eigenvalues. The results of *h*-version of CEM for the first beam eigenvalues are alike those obtained by the *h*-version of GFEM. However the higher beam eigenvalues obtained by the *h*-version of GFEM are more precise.

The *p*-version of GFEM is quite accurate and its convergence rates are higher than those obtained by the *h*-versions of FEM and the *c*-version of CEM in free vibration analysis of bars and beams. It is observed however that the last eigenvalues obtained in each analysis of *p*-version of GFEM did not show good accuracy, but this deficiency is also found in the other enriched methods, such as the CEM. Although the *p* refinement of GFEM has produced excellent results and convergence rates, the adaptive GFEM exhibits special skills to reach accurately a specific frequency.

In most of the free vibration analysis it is virtually impossible to get all the natural frequencies. However, in practical analysis it is sufficient to work with a set of frequencies in a range (or band), or with those which have more significant participation in the analysis. The adaptive GFEM allows to find a specific natural frequency with accuracy and computational efficiency. It may be used in repeated analyses in order to find all the frequency in the range of interest.

In the C^0 adaptive GFEM, trigonometric enrichment functions depending on geometric and mechanical properties of the elements are added to the linear FEM shape functions by the partition of unity approach. This technique allows an accurate adaptive process that converges very fast and is able to refine the frequency related to a specific vibration mode. The adaptive GFEM shows fast convergence and remains stable after the third iteration with quite precise results for the target frequency.

The results have shown that the adaptive GFEM is more accurate than the *h* refinement of FEM and the *c* refinement of CEM, both employing a larger number of degrees of freedom. The adaptive GFEM in free vibration analysis of bars has exhibited similar accuracy, in some cases even better, to those obtained by the *p* refinement of FEM.

Thus the adaptive GFEM has shown to be efficient in the analysis of longitudinal vibration of bars, so that it can be applied, even for a coarse discretization scheme, in complex practical problems. Future research will extend this adaptive method to other structural elements like beams, plates and shells.

7. References

Abdelaziz, Y. & Hamouine, A. (2008). A survey of the extended finite element. *Computers and Structures*, Vol. 86, 1141-1151.

Arndt, M.; Machado, R.D. & Scremin A. (2010). An adaptive generalized finite element method applied to free vibration analysis of straight bars and trusses. *Journal of Sound and Vibration*, Vol. 329, 659–672.

Babuska, I. ; Banerjee, U. & Osborn, J.E. (2004). Generalized finite element methods: main ideas, results, and perspective. *Technical Report 04-08*, TICAM, University of Texas at Austin.

Carey, G.F. & Oden, J.T. (1983). *Finite elements: A second course*, Vol. 2, Prentice -Hall, New Jersey.

Carey, G.F. & Oden, J.T. (1984). *Finite elements: Computational aspects*, Vol. 3, Prentice -Hall, New Jersey.

Craig, R.R. (1981). *Structural dynamics: an introduction to computer methods*, John Wiley, New York.

De, S. & Bathe, K.J. (2001). The method of finite spheres with improved numerical integration. *Computers and Structures*, Vol. 79, 2183-2196.

De Bel, E.; Villon, P. & Bouillard, Ph. (2005). Forced vibrations in the medium frequency range solved by a partition of unity method with local information. *International Journal for Numerical Methods in Engineering*, Vol. 62, 1105-1126.

Duarte, C.A.; Babuska, I. & Oden, J.T. (2000). Generalized finite element methods for three-dimensional structural mechanics problems. *Computers and Structures*, Vol. 77, 215-232.

Duarte, C.A. & Kim, D-J. (2008). Analysis and applications of a generalized finite element method with global-local enrichment functions. *Computer Methods in Applied Mechanics and Engineering*, Vol. 197, 487-504.

Duarte, C.A. & Oden, J.T. (1996). An *h-p* adaptive method using clouds. *Computer Methods in Applied Mechanics and Engineering*, Vol. 139, 237-262.

Engels, R.C. (1992). Finite element modeling of dynamic behavior of some basic structural members. *Journal of Vibration and Acoustics*, Vol. 114, 3-9.

Ganesan, N. & Engels, R.C. (1992). Hierarchical Bernoulli-Euller beam finite elements. *Computers & Structures*, Vol. 43, No. 2, 297-304.

Gartner, J.R. & Olgac, N. (1982). Improved numerical computation of uniform beam characteristic values and characteristic functions. *Journal of Sound and Vibration*, Vol. 84, No. 4, 481-489.

Gracie, R.; Ventura, G. & Belytschko, T. (2007) A new fast finite element method for dislocations based on interior discontinuities. *International Journal for Numerical Methods in Engineering*, Vol. 69, 423-441.

Hazard, L. & Bouillard, P. (2007). Structural dynamics of viscoelastic sandwich plates by the partition of unity finite element method. *Computer Methods in Applied Mechanics and Engineering*, Vol. 196, 4101-4116.

Khoei, A.R.; Anahid, M. & Shahim, K. (2008). An extended arbitrary Lagrangian-Eulerian finite element method for large deformation of solid mechanics. *Finite Elements in Analysis and Design*, Vol. 44, 401-416.

Kumar, B.M. & Sujith, R.I. (1997). Exact solutions for the longitudinal vibration of non-uniform rods. *Journal of Sound and Vibration*, Vol. 207, 721-729.

Leung, A.Y.T. & Chan, J.K.W. (1998). Fourier *p*-element for the analysis of beams and plates. *Journal of Sound and Vibration*, Vol. 212, No. 1, 179-185.

Lu, Z.R. & Law, S.S. (2007). Discussions on composite element method for vibration analysis of structure. *Journal of Sound and Vibration*, Vol. 305, 357-361.

Melenk, J.M. & Babuska, I. (1996). The partition of unity finite element method: basic theory and applications. *Computer Methods in Applied Mechanics and Engineering*, Vol. 139, No. 1-4, 289-314.

Nistor, I.; Pantalé, O. & Caperaa, S. (2008). Numerical implementation of the extended finite element method for dynamic crack analysis. *Advances in Engineering Software*, Vol. 39, 573-587.

Oden, J.T.; Duarte, C.A.M. & Zienkiewicz, O.C. (1998). A new cloud-based hp finite element method. *Computer Methods in Applied Mechanics and Engineering*, Vol. 153, 117-126.

Schweitzer, M.A. (2009). An adaptive hp-version of the multilevel particle-partition of unity method. *Computer Methods in Applied Mechanics and Engineering*, Vol. 198, No. 13-14, 1260-1272.

Sukumar, N.; Chopp, D.L.; Moes, N. & Belytschko, T. (2001). Modeling holes and inclusions by level sets in the extended finite-element method. *Computer Methods in Applied Mechanics and Engineering*, Vol. 190, 6183-6200.

Sukumar, N.; Moes, N.; Moran, B. & Belytschko, T. (2000). Extended finite element method for three-dimensional crack modeling. *International Journal for Numerical Methods in Engineering*, Vol. 48, 1549-1570.

Strouboulis, T.; Babuska, I. & Copps, K. (2000). The design and analysis of the generalized finite element method. *Computer Methods in Applied Mechanics and Engineering*, Vol. 181, 43-69.

Strouboulis, T.; Babuska, I. & Hidajat, R. (2006a). The generalized finite element method for Helmholtz equation: theory, computation and open problems. *Computer Methods in Applied Mechanics and Engineering*, Vol. 195, 4711-4731.

Strouboulis, T.; Copps, K. & Babuska, I. (2001). The generalized finite element method. *Computer Methods in Applied Mechanics and Engineering*, Vol. 190, 4081-4193.

Strouboulis, T.; Hidajat, R. & Babuska, I. (2008). The generalized finite element method for Helmholtz equation. Part II: effect of choice of handbook functions, error due to absorbing boundary conditions and its assessment. *Computer Methods in Applied Mechanics and Engineering*, Vol. 197, 364-380.

Strouboulis, T.; Zhang, L.; Wang, D. & Babuska, I. (2006b). A posteriori error estimation for generalized finite element methods. *Computer Methods in Applied Mechanics and Engineering*, Vol. 195, 852-879.

Xiao, Q.Z. & Karihaloo, B.L. (2007). Implementation of hybrid crack element on a general finite element mesh and in combination with XFEM. *Computer Methods in Applied Mechanics and Engineering*, Vol. 196, 1864-1873.

Zeng, P. (1998a). Composite element method for vibration analysis of structures, part I: principle and C^0 element (bar). *Journal of Sound and Vibration*, Vol. 218, No. 4, 619-658.

Zeng, P. (1998b). Composite element method for vibration analysis of structures, part II: C^1 element (beam). *Journal of Sound and Vibration*, Vol. 218, No. 4, 659-696.

Zeng, P. (1998c). Introduction to composite element method for structural analysis in engineering. *Key Engineering Materials*, Vol. 145-149, 185-190.

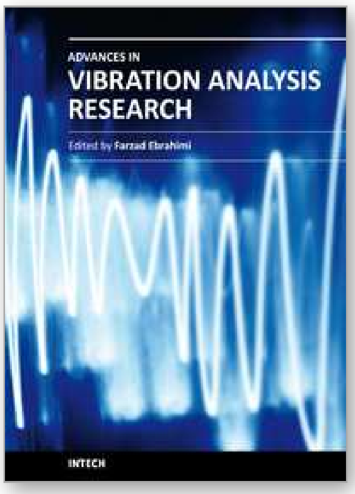

ISBN 978-953-307-209-8
Hard cover, 456 pages
Publisher InTech
Published online 04, April, 2011
Published in print edition April, 2011